JOURNAL OF CATALYSIS **177,** 217–223 (1998)
ARTICLE NO. CA982101

Decomposition of N_2O on Ni(755) and the Character of the Atomic Oxygen Deposited at Step Sites

Hideo Orita, Hiroshi Kondoh, and Hisakazu Nozoye[1]

National Institute of Materials and Chemical Research, Tsukuba, Ibaraki 305, Japan

Received November 18, 1997; revised April 10, 1998; accepted April 10, 1998

Adsorption and reaction of N_2O on a stepped Ni(755) surface have been investigated by temperature-programmed desorption (TPD). The decomposition of adsorbed N_2O occurs exclusively at the step sites on Ni(755) below 200 K during TPD ramp, yielding gaseous N_2 and leaving atomic oxygen there. The amount of the atomic oxygen is controlled easily by changing the exposure of N_2O. The character of the atomic oxygen has been studied by using decomposition of cycloheptane as a probe reaction. All the atomic oxygen generated *in situ* from coadsorbed N_2O can react with carbon atoms produced from the decomposition of cycloheptane, resulting in desorption of CO around 600 K upon heating. However, two thirds of the predeposited atomic oxygen cannot be desorbed as CO upon heating up to 723 K. The predeposited atomic oxygen becomes inactive during the predeposition process and probably interacts with the step sites more strongly.

1. INTRODUCTION

The study of nitrogen oxides is important to combustion processes such as in automobile engines, where nitrogen oxides are potential poisons for catalysts as well as atmospheric pollutants. Among nitrogen oxides, decomposition of N_2O has been studied on a wide variety of surfaces and under various experimental conditions because of its simplicity. Recently, the study of N_2O has gained more significance because N_2O contributes to the catalytic decomposition of stratospheric ozone and is a greenhouse gas. N_2O is also a good molecule as a precursor of atomic oxygen and can be used as a selective oxidizing reagent of methane to methanol (1). There are several investigations concerning adsorption and reaction of N_2O on metal surfaces under ultra-high vacuum conditions. For example, Umbach and Menzel (2) have studied the adsorption of N_2O on W(110) and Ru(001) by means of XPS and UPS, and they have reported that adsorption on clean Ru(001) at 83 K yields a simultaneous buildup of dissociated oxygen and molecular N_2O. For fcc metals, N_2O does not decompose on (111) surfaces such as Pt (3), Ir (4), Rh (5), and Ni (6). Decomposition of N_2O is observed on Ni(100) (7), Ni(110) (8), and Rh(110) (5) by using molecular beam technique, but the decomposition on Ni(100) occurs only at temperatures above 200 K (7). These studies indicate that the decomposition of N_2O is very dependent on kinds and surface orientations of metals. It is interesting to know how step sites work on the decomposition of N_2O because step sites are considered to be active sites for various catalytic reactions (9). However, there is no investigation about an effect of step sites on the decomposition of adsorbed N_2O as far as we know.

In the present work, we have studied the adsorption and reaction of N_2O on a stepped Ni(755) {Ni[6(111) × (100)]} by temperature-programmed desorption (TPD) to examine effects of the steps on the decomposition of adsorbed N_2O. The results indicate that the decomposition of adsorbed N_2O occurs easily at the step sites below 200 K to yield gaseous N_2 and atomic oxygen on the surface. We can easily control the amount of the atomic oxygen adsorbed at the step sites by changing the exposure of N_2O. We have also investigated the character of the atomic oxygen by using decomposition of hydrocarbons as a probe reaction. Decomposition of hydrocarbons on metal surfaces is widely investigated and well known as a structure-sensitive reaction (9), so the decomposition property of hydrocarbons should be dependent on the character of the atomic oxygen. Among various hydrocarbons we choose cycloheptane as a probe molecule because we have found previously that cycloheptane is a good example of hydrocarbons which decompose efficiently on Ni(755) (10). The character of the atomic oxygen is dependent on the way to produce the atomic oxygen.

2. EXPERIMENTAL

All the experiments were conducted in a stainless steel ultra-high vacuum system equipped with a single-pass CMA for Auger electron spectroscopy (AES), four-grid low-energy electron diffraction (LEED) optics, a

[1] To whom correspondence should be addressed. E-mail: nozoye@nimc.go.jp.

0021-9517/98 $25.00

quadrupole mass spectrometer (QMS) for TPD and an ion gun for cleaning. The base pressure was less than 1×10^{-10} Torr (1 Torr = 133.3 Pa). A disk-shaped Ni(755) crystal (ca ϕ 8 × 1 mm) was heated resistively and cooled down to 90 K. The sample temperature was measured by a chromel–alumel thermocouple spot-welded to the edge of the crystal. The Ni(755) surface was cleaned by Ar-ion sputtering followed by annealing to 1080 K. Cleanliness and ordering of the surface were checked by AES and LEED.

Exposure of gases on the surface was performed using a gas doser which was composed of a glass capillary array. The exposure was controlled by varying dose time and back pressure of the doser (usually 1×10^{-4} Torr, which was not corrected for ion gauge sensitivity to various gases). TPD experiments were carried out with a linear heating rate of 10 K/s controlled by a personal computer. Four masses were monitored simultaneously in a single experiment and the data were stored in the computer. The coverage of adsorbed CO relative to a surface Ni atom was determined from the integrated mass intensity of TPD peak, assuming that the saturation coverage around 300 K is 0.5 monolayer (ML) (11). In the present experimental conditions, the saturation coverage of CO around 300 K (i.e., 0.5 ML) was accomplished at a dose time of 50 s.

Cycloheptane was purchased and purified by freeze-pump-thaw cycles for at least five times. The hydrogen, N_2O, and CO were research grade purity and used without further purification. Purity of all the gases were verified by mass spectroscopy after admission into the ultra-high vacuum chamber.

3. RESULTS AND DISCUSSION

3.1. Decomposition of N_2O on Clean Ni(755)

Adsorption and reaction of N_2O on Ni(755) were studied by TPD. Figures 1a and 1b show a series of TPD spectra of N_2 ($m/e = 28$) and N_2O ($m/e = 44$), respectively, after adsorption of N_2O on Ni(755) at 113 K. Figure 2 exhibits the TPD peak areas of N_2 ($m/e = 28$) and N_2O ($m/e = 44$) with N_2O dose time. We did not detect any desorption of NO and O_2. The TPD spectra of N_2 were characterized by the presence of a main peak at 171–175 K and a shoulder at around 145 K. Their peak positions changed little with dose time. Figure 2 clearly shows that the peak area of N_2 increased linearly with increase of dose time and was saturated by a dose time of ca 50 s. The gradual increase of the peak area for dose times $\geq$60 s came from the fragment of molecular N_2O. (The contribution from the fragment of N_2O to the N_2 peak area could be easily eliminated by subtracting 0.25 times of the N_2O peak area from the N_2 peak area; the fragment ratio of N_2 to N_2O was 0.25 for our QMS.) Desorption of N_2O (Fig. 1b) was observed for dose times >30 s with peak areas much less than one-tenth of N_2 (cf. Fig. 2). The peak of N_2O appeared from the starting temperature of TPD run (113 K) and centered around 130 K with a tail extending to 180 K. The peak area of N_2O was not saturated by a dose time of 105 s. After TPD measurements, AES revealed the presence of oxygen but not nitrogen on the surface. These results show that all the N_2O adsorbed on Ni(755) was decomposed to gaseous N_2 and atomic oxygen below 200 K for does times <30 s. The existence of two

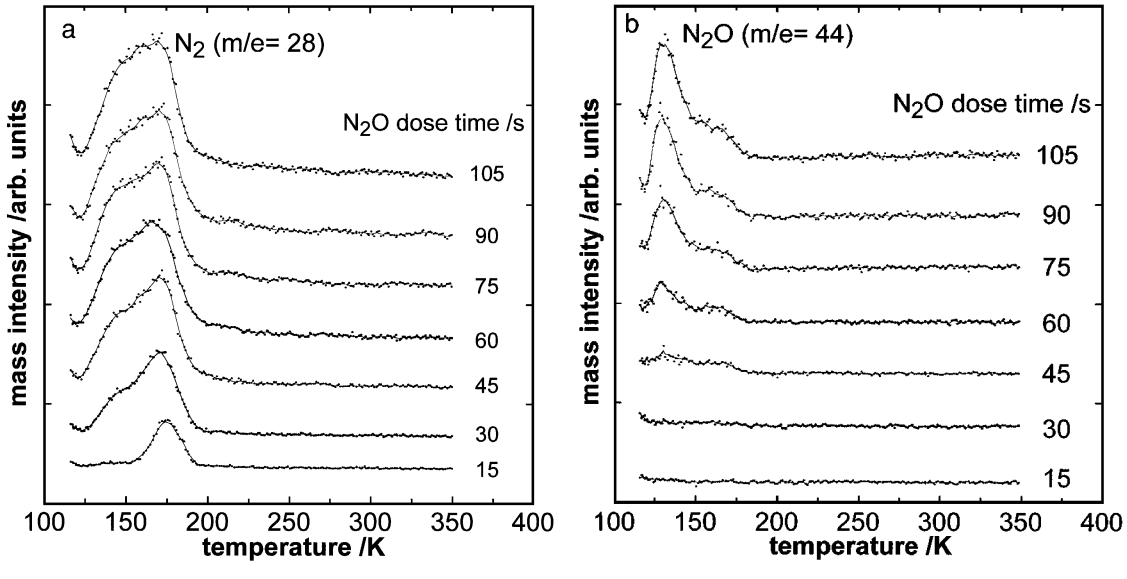

FIG. 1. TPD spectra for the desorption of (a) N_2 ($m/e = 28$) and (b) N_2O ($m/e = 44$) after adsorption of N_2O on Ni(755) at 113 K as a function of N_2O dose time.

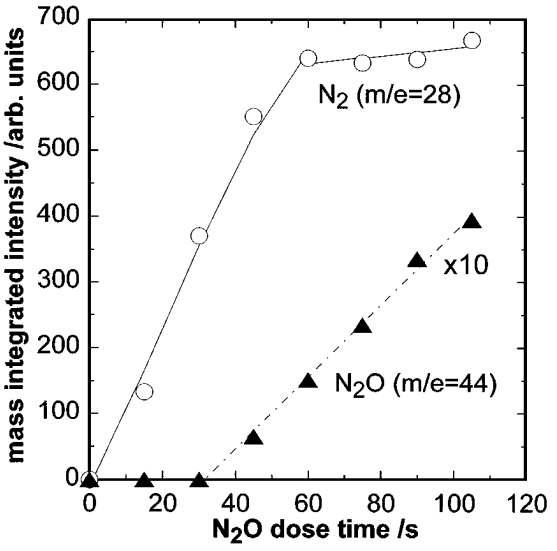

FIG. 2. Variations in TPD peak areas of N_2 ($m/e = 28$) and N_2O ($m/e = 44$) with N_2O dose time. N_2O was dosed to clean Ni(755) at 113 K before TPD spectra were measured.

desorption peaks of N_2 suggests that there were different decomposition pathways of N_2O. Assignment of N_2 desorption peaks by means of XPS as well as TPD will be reported elsewhere (12).

We estimated the amount of N_2 from the TPD peak area, where the mass sensitivity factor for N_2 is assumed to be equal to that for CO. The amount of N_2 for an N_2O dose time of 60 s (the saturation of N_2 production) was determined from Fig. 2 to be 0.17 ± 0.02 ML. The amount of the atomic oxygen deposited on the surface from the decomposition of N_2O was equal to that of N_2 because any desorption of oxygenated compounds such as O_2 and NO was not detected.

The step density (the ratio of step edge atoms to exposed surface atoms) is one-sixth for Ni(755). The amount of the saturated N_2 production (0.17 ML) was quite close to the step density of Ni(755), suggesting that the decomposition of N_2O occurred exclusively at the step sites and adsorption sites of atomic oxygen were limited to the step sites. This deduction seems rational because Vaterlein *et al.* recently shows that N_2O does not decompose efficiently on Ni(111) (6). In addition, the oxygen atom is chemisorbed at the fcc threefold hollow site for Ni(111) (the terrace of Ni(755)) and the fourfold hollow site for Ni(100) (the step of Ni(755)) (13). The ratio of the fourfold hollow sites on the step to the surface nickel atoms is also one-sixth for Ni(755).

We have previously studied the dissociated adsorption of NO on Ni(755) (14) and found that not only oxygen but also nitrogen atoms are selectively adsorbed along the step sites at low exposures of NO. Winkler and Rendulic (15) have also reported that the oxygen atom from O_2 is preferentially adsorbed at the step sites of Ni(977) at oxygen coverages ≤ 0.05 ML. However, the oxygen atom from NO or O_2 is adsorbed also on the terrace at large exposures of NO or O_2. For N_2O, the adsorption sites of the atomic oxygen were limited to the step sites. We could control the coverage of atomic oxygen at the step sites by changing the exposure of N_2O as shown in Fig. 2.

3.2. Effects of Predeposited Atomic Oxygen on Decomposition of Cycloheptane

To investigate the effects of the predeposited atomic oxygen at the step sites on the decomposition of cycloheptane, TPD spectra were measured after adsorption of cycloheptane on the surface at 123 K with varying amounts of predeposited atomic oxygen. The predeposited atomic oxygen was prepared by the decomposition of adsorbed N_2O with flashing to 248 K at a rate of 10 K/s. The amount of the deposited atomic oxygen was estimated from that of N_2 produced from the decomposition of N_2O. We used a mass peak of $m/e = 55$ to monitor cycloheptane since the fragment peak was much more intense than the parent peak ($m/e = 98$); we assured that its behavior was equivalent to that of the parent peak. Water and any product other than hydrogen were not detected by TPD in all the experiments. The H_2 TPD spectra were not corrected for the adsorbed hydrogen from the residual gas in our UHV system.

Typical TPD spectra for adsorption of cycloheptane on an O-predeposited surface at an oxygen coverage of 0.11 ML are presented in Fig. 3. Hydrogen ($m/e = 2$) was desorbed in a broad feature from 250 to 500 K. The evolution of hydrogen indicated that some of the adsorbed cycloheptane were

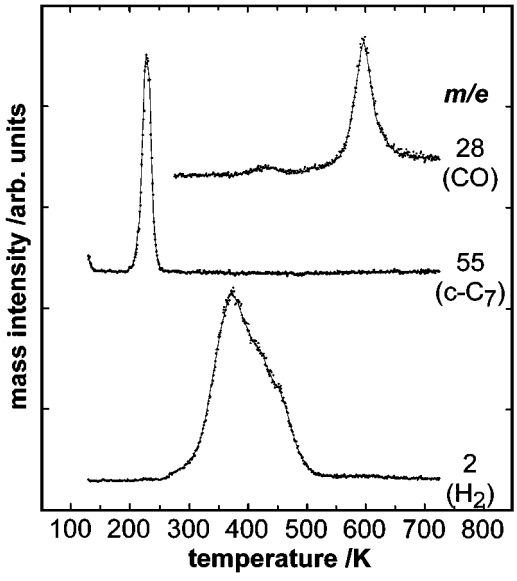

FIG. 3. Typical TPD spectra for adsorption of cycloheptane at 123 K on the O-predeposited surface at a coverage of 0.11 ML. N_2O was predosed for 30 s to clean Ni(755) at 113 K and the surface was flashed at 10 K/s to 248 K to produce the O-predeposited surface. After cooling to 123 K, cycloheptane was postdosed to the surface for 80 s and then TPD spectrum was measured.

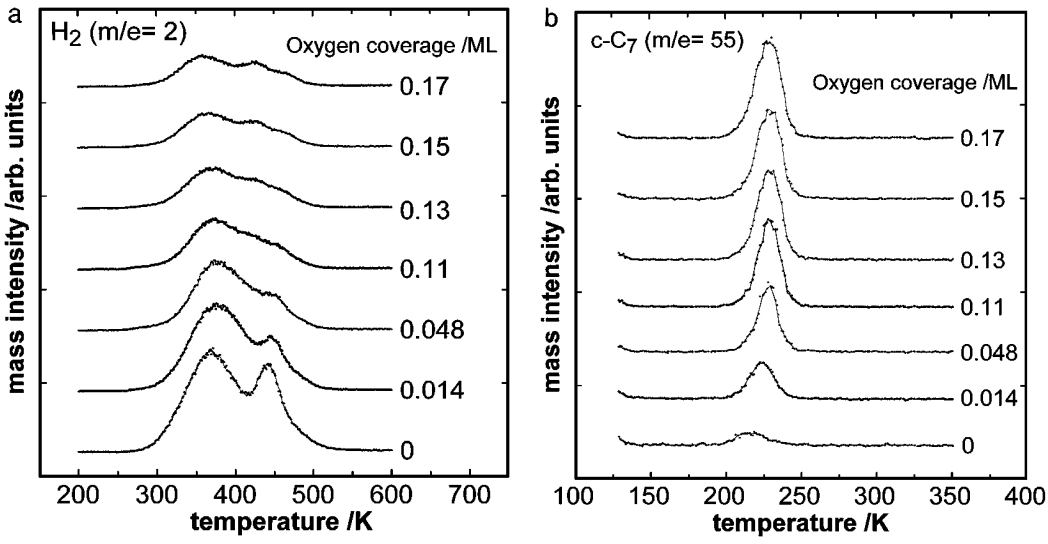

FIG. 4. Variations in TPD spectra for (a) hydrogen ($m/e = 2$) and (b) cycloheptane ($m/e = 55$) on the amount of the predeposited oxygen atom. N_2O was predosed for various N_2O dose times to clean Ni(755) at 113 K and the surface was flashed at 10 K/s to 248 K to produce atomic oxygen on the surface. After cooling to 123 K, cycloheptane was postdosed to the surface for 80 s and then TPD spectrum was measured.

dehydrogenated on the O-predeposited surface. Molecular cycloheptane ($m/e = 55$) gave a single desorption peak at 229 K. For the signal at $m/e = 28$, two peaks were observed at around 450 and 600 K. The small peak at around 450 K was due to the desorption of molecular CO which was inevitably adsorbed from the residual gas. The peak at around 600 K was observed only in the presence of both the atomic oxygen and the coadsorbed cycloheptane. Referring the previous reports (16, 17), the peak at around 600 K was assigned to the associative desorption of CO by combination of the predeposited atomic oxygen and carbon atoms from the decomposition of cycloheptane.

The variations in TPD spectra for hydrogen ($m/e = 2$) and cycloheptane ($m/e = 55$) with the amount of predeposited atomic oxygen are indicated in Figs. 4a and 4b, respectively (the dose time of cycloheptane was fixed at 80 s in this experiment). On increase of the amount of predeposited atomic oxygen, the peak of hydrogen decreased in intensity with changing its peak shape, which indicated that the predeposited atomic oxygen suppressed the decomposition of cycloheptane. Two peaks were observed clearly in the absence of predeposited atomic oxygen. As discussed previously (10), the low temperature peak of hydrogen was due to the associative desorption of adsorbed hydrogen atoms arising from the dehydrogenation of cycloheptane, and the high temperature peak was the reaction-limited desorption due to the decomposition of reaction intermediates. The high temperature peak at around 450 K decreased rapidly with increase of the amount of predeposited atomic oxygen. Three peaks were observed clearly in the presence of larger amount of predeposited atomic oxygen. The peak of cycloheptane increased in intensity and shifted to higher temperature from 219 to 229 K with increase of the amount of predeposited atomic oxygen, showing that cycloheptane was stabilized in the presence of atomic oxygen. This result is consistent with reflection–absorption infrared spectroscopy (RAIRS) studies on coadsorption of oxygen and cyclohexane on Ni(111) which show that the charge transfer from the filled CH σ orbital to the metal is enhanced at low coverages of oxygen (18). When only cycloheptane was adsorbed on clean Ni(755), the peak of cycloheptane shifted to lower temperature from 232 to 202 K with increase of cycloheptane coverage (10), which was associated with an intermolecular repulsive interaction between cycloheptane molecules. Therefore, it is considered that the oxygen-induced stabilization is stronger than the destabilization due to the repulsive interaction between cycloheptane molecules.

Figure 5 shows the dependence of TPD peak areas of H_2, CO, and cycloheptane on the amount of the predeposited atomic oxygen. The peak position of CO was not very dependent on the amount of the predeposited atomic oxygen. The amount of the associative desorption of CO was equal to that of the predeposited atomic oxygen up to 0.05 ML and leveled off above a coverage of 0.05 ML. The peak area of hydrogen decreased greatly but not linearly with increasing the amount of the predeposited atomic oxygen up to 0.17 ML (the peak area of hydrogen at an oxygen coverage of 0.17 ML was still larger than that of the hydrogen adsorbed from the residual gas (about 100 for the unit in Fig. 5)). The fast saturation of CO peak area and the nonlinear decrease of H_2 peak area suggested that the predeposited atomic oxygen was not uniform in character. There was a good mass balance between the decrease of hydrogen

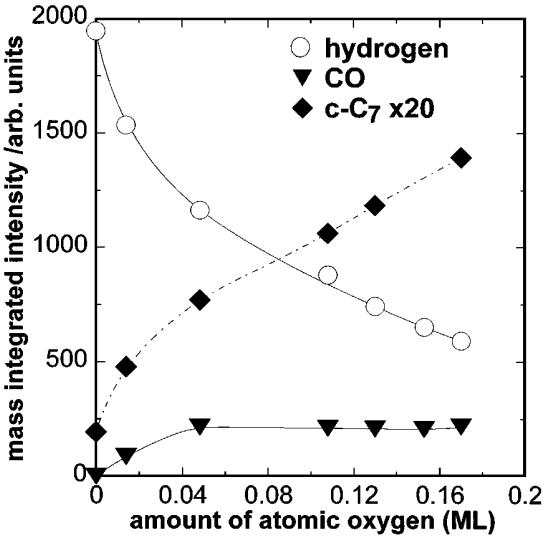

FIG. 5. Dependence of TPD peak areas of H_2 ($m/e = 2$), CO ($m/e = 28$), and cycloheptane ($m/e = 55$) on the amount of the predeposited oxygen atom. N_2O was predosed for various N_2O dose times to clean Ni(755) at 113 K and the surface was flashed at 10 K/s to 248 K to produce atomic oxygen on the surface. After cooling to 123 K, cycloheptane was postdosed to the surface for 80 s and then TPD spectrum was measured. From the mass balance between hydrogen and cycloheptane, the amount of adsorbed cycloheptane was determined to be 0.05 ± 0.005 ML (see text).

and the increase of cycloheptane as described below, showing that the decrease of hydrogen was due to the suppression of the decomposition of cycloheptane by the atomic oxygen and that both hydrogen and cycloheptane did not react to the predeposited atomic oxygen considerably. In fact, we observed neither the production of water nor other gaseous products. Winkler and Rendulic have reported that there is no reaction between hydrogen and oxygen on Ni(111); the hydrogen on Ni(111) is desorbed around 400 K before reacting with the adsorbed oxygen (15).

We could determine the mass sensitivity factor for hydrogen from TPD for H_2 adsorption. It is known (19) that hydrogen molecules adsorb dissociatively on Ni(755) and the saturation coverage of adsorbed hydrogen atom is 1 ML. The amount of decomposed cycloheptane was estimated from that of evolved hydrogen. We could calibrate the mass sensitivity factor for molecular cycloheptane ($m/e = 55$) by using the TPD peak areas of both hydrogen and cycloheptane since the mass balance between hydrogen and cycloheptane was conserved in Fig. 5. Thus, the amount of cycloheptane which was desorbed molecularly was estimated on the basis of this sensitivity factor. The amount of adsorbed cycloheptane (i.e., the sum of decomposed and desorbed cycloheptane) in Fig. 5 was determined to be 0.050 ± 0.005 ML for all the oxygen coverages. The decomposition fraction (ratio of decomposed molecules to adsorbed ones) without the predeposited atomic oxygen in Fig. 5 was 0.89 ± 0.05. The minimum of the decomposition fraction, at an oxygen coverage of 0.17 ML, was 0.28. The decomposition of cycloheptane could not be suppressed completely even in the presence of the maximum amount of the predeposited atomic oxygen, suggesting that the oxygen-modified step sites might have some activity for the decomposition of cycloheptane.

3.3. Effects of Coadsorbed N_2O on Decomposition of Cycloheptane

TPD spectra were measured after cycloheptane was dosed at a fixed dose time (80 s) to clean Ni(755) at 113 K, followed by exposure to various amounts of N_2O. Typical TPD spectra for coadsorption of cycloheptane and N_2O are presented in Fig. 6 (N_2O dose time = 80 s). Hydrogen ($m/e = 2$) was desorbed in a broad feature from 250 to 500 K. A desorption peak of N_2O ($m/e = 44$) appeared from the starting temperature of TPD run (113 K) and was centered around 130 K (the small peak around 220 K was a fragment peak of cycloheptane) as observed for the adsorption of N_2O on clean Ni(755) in Fig. 1b. Molecular cycloheptane ($m/e = 55$) gave a single desorption peak at 223 K. For the signal at $m/e = 28$, two peaks were observed clearly at around 150 and 600 K. The low temperature peak below 200 K was assigned to the desorption of N_2 from the decomposition of N_2O (a hump structure around 220 K came from a fragment of cycloheptane in the QMS). The peak position of N_2 shifted to lower temperature (ca 150 K) in the presence of coadsorbed cycloheptane (cf. Fig. 1a). The peak at around 600 K was assigned to the associative desorption of CO by combination of oxygen and carbon atoms. The amount of CO was equal to that of N_2. The TPD spectra in Fig. 6 clearly indicate that both desorption and decomposition of N_2O were finished and atomic oxygen was

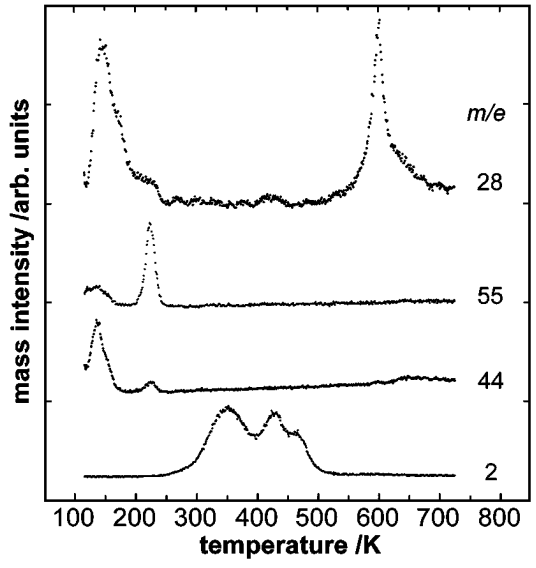

FIG. 6. Typical TPD spectra for the coadsorption of cycloheptane and N_2O on Ni(755) at 113 K. Cycloheptane was predosed to clean Ni(755) at 113 K for 80 s and then N_2O was postdosed for 80 s.

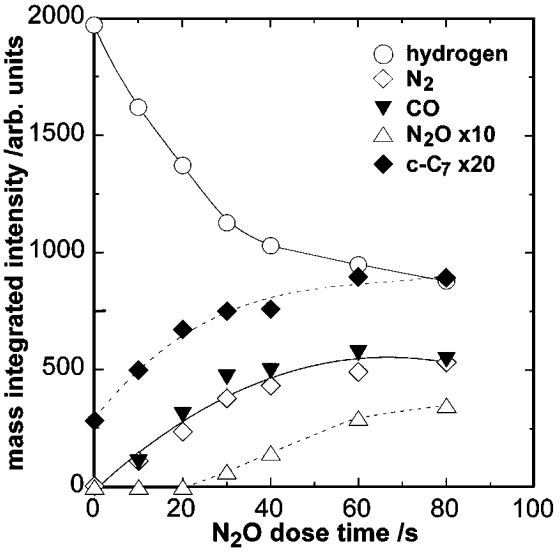

FIG. 7. Dependence of TPD peak areas of H_2 ($m/e=2$), N_2 ($m/e=28$), CO ($m/e=28$), N_2O ($m/e=44$), and cycloheptane ($m/e=55$) on N_2O dose time. Cycloheptane was predosed to clean Ni(755) at 113 K for 80 s and then N_2O was postdosed for various dose times. From the mass balance between hydrogen and cycloheptane, the amount of adsorbed cycloheptane was determined to be 0.056 ± 0.005 ML.

deposited on the surface before the desorption of molecular cycloheptane started from 200 K. The amount of the atomic oxygen generated from coadsorbed N_2O was estimated to be 0.13 ML from that of evolved N_2 in Fig. 6.

The variations in TPD spectra for hydrogen and cycloheptane with N_2O dose time were similar to those in Figs. 4a and 4b, respectively (spectra not shown). On increase of N_2O dose time, the peak of hydrogen decreased in intensity with changing its peak shape. The peak of cycloheptane increased in intensity and the peak position shifted from 218 to 223 K. Figure 7 shows the dependence of TPD peak areas of H_2, N_2, CO, N_2O, and cycloheptane on N_2O dose time (the dose time of cycloheptane was fixed at 80 s). In comparison with the results of N_2O on the clean surface in Fig. 2, the amount of N_2 in Fig. 7 was a little smaller than that in Fig. 2 at the same dose time (e.g., the amounts of saturated N_2 production at an N_2O dose time of 60 s in Figs. 2 and 7 were 0.17 and 0.13 ML, respectively). On the contrary, the amount of N_2O in Fig. 7 was larger than that in Fig. 2. These results indicate that the coadsorbed cycloheptane suppressed partially the decomposition of N_2O by competitive adsorption at the step sites. The amount of CO was always equal to that of N_2, showing that all the atomic oxygen reacted to carbon atoms and was desorbed as CO from the surface upon heating.

The peak area of hydrogen decreased sharply with increase of N_2O dose time up to 30 s (the amount of the atomic oxygen generated at this dose time was 0.10 ML), and the gradual decrease of the hydrogen was observed on further increase of N_2O dose time. The peak area of cycloheptane increased with the behavior reversed to that of hydrogen, and the decrease of hydrogen correlated linearly with the increase of cycloheptane. The suppression of the decomposition of cycloheptane was observed even at a short dose time of 10 s (all the adsorbed N_2O was decomposed to gaseous N_2 and atomic oxygen for short dose times $\leq$20 s, and the amounts of the atomic oxygen generated were 0.03 and 0.06 ML at N_2O dose times of 10 and 20 s, respectively). These results showed that the generated atomic oxygen at a small coverage of 0.03 ML blocked the pathway for the decomposition of cycloheptane at bare step sites. The amount of adsorbed cycloheptane in Fig. 7 was determined to be 0.056 ± 0.005 ML for all the N_2O dose time as shown in Fig. 5. The decomposition fraction at zero N_2O dose time was 0.79 ± 0.05. The minimum decomposition fraction in Fig. 8 was 0.37.

3.4. Comparison of the Character of Two Atomic Oxygen Species (the Predeposited Atomic Oxygen and the Atomic Oxygen Generated during TPD Ramp)

We compared the effects of the production methods of atomic oxygen species on the decomposition of cycloheptane (the predeposited atomic oxygen and the atomic oxygen generated during TPD ramp). TPD peak areas of H_2 and CO in Figs. 5 and 7 were replotted as shown in Fig. 8

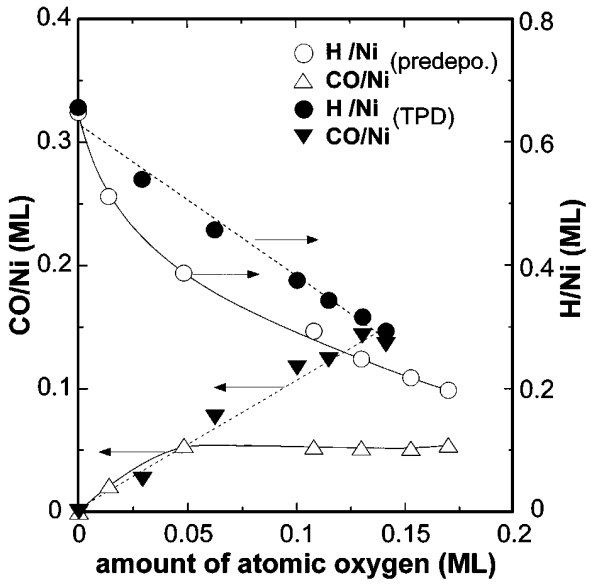

FIG. 8. Comparison of the effects of the two atomic oxygen species from the decomposition of N_2O (the predeposited atomic oxygen and the atomic oxygen produced during TPD ramp) on the decomposition of cycloheptane. TPD peak areas of H_2 and CO which are scaled to the ratios relative to the surface nickel atoms (H/Ni and CO/Ni) are plotted against the amount of the atomic oxygen, which was calculated from the amount of N_2 evolved from the decomposition of N_2O. The details of the experiments for the predeposited atomic oxygen and the atomic oxygen produced during TPD ramp are shown in the captions in Figs. 5 and 7, respectively.

against the amount of the atomic oxygen, which was estimated from the amount of N_2 produced from the decomposition of N_2O. In this figure, TPD peak areas are scaled to the ratios relative to the surface nickel atoms (H/Ni or CO/Ni). These values were derived by means of calibration of the QMS described above. This figure clearly indicates that the characters of two atomic oxygen species are different, as mentioned below.

For the atomic oxygen generated during TPD ramp, the evolved hydrogen (H/Ni) decreased almost linearly with the increase of the amount of atomic oxygen at a slope of 2.5. On the other hand, the decrease of the evolved hydrogen (H/Ni) was quite nonlinear with the increase of the amount of predeposited atomic oxygen. In this case, the initial slope at the limit of zero coverage of atomic oxygen was about 10. The predeposited atomic oxygen at the limit of its zero coverage suppressed the decomposition of cycloheptane more effectively than the atomic oxygen generated during TPD ramp.

The amount of the associative desorption of CO from the atomic oxygen generated during TPD ramp was always equal to the amount of the atomic oxygen. All the atomic oxygen generated during TPD ramp had the same reactivity to carbon atoms. However, about two-thirds of the predeposited atomic oxygen could not be desorbed as CO upon heating up to 723 K. The predeposited atomic oxygen became inactive during the predeposition process, i.e., flashing and quenching. For the atomic oxygen generated during TPD ramp, the presence of coadsorbed species produced from decomposition of cycloheptane might prevent this inactivation path.

The change in reactivity of adsorbed oxygen atom by annealing has been reported for Cu(110) by Sueyoshi *et al.* (20). They have found that the as-exposed oxygen on Cu(110) at 100 K oxidizes CO to CO_2 while oxygen atoms after annealing above 200 K are inactive. They have also observed the change of adsorbed oxygen from the as-exposed structure to the (2×1)-O phase upon annealing above 200 K by HREELS. They have concluded that the as-exposed oxygen atoms in no ordered structure are more reactive than the oxygen atoms in the (2×1)-O phase. In the present work, the atomic oxygen generated from coadsorbed N_2O during TPD ramp showed higher reactivity to carbon atoms than the predeposited atomic oxygen. This difference in reactivity probably comes from the difference in adsorbed state of two oxygen species.

4. SUMMARY

The N_2O adsorbed on Ni(755) decomposed below 200 K during TPD ramp. N_2 was desorbed and atomic oxygen was deposited on the surface upon heating. The amount of evolved N_2 was saturated at 0.17 ML. This value was quite close to the step density of Ni(755) (one-sixth), which suggested that N_2O was decomposed at the step sites.

The predeposited atomic oxygen suppressed the decomposition of cycloheptane effectively, indicating that the atomic oxygen, which was adsorbed on the step, blocked the decomposition pathway at bare step sites. Only one-third of the predeposited atomic oxygen could react with carbon atoms from decomposition of cycloheptane, resulting in desorption of CO around 600 K upon heating up to 723 K. This is because some of the atomic oxygen became inactive during the predeposition process, i.e., flashing to 248 K and quenching.

For coadsorption of cycloheptane and N_2O, the atomic oxygen generated during TPD ramp suppressed the decomposition of cycloheptane linearly but less effectively than the predeposited atomic oxygen. All of the atomic oxygen generated during TPD ramp was desorbed as CO around 600 K by combination with carbon atoms produced from the decomposition of cycloheptane. The character of the atomic oxygen generated during TPD ramp was nearly uniform. The above difference in character of two atomic oxygen species is probably due to the difference in their adsorbed state.

REFERENCES

1. Pitchai, R., and Klier, K., *Catal. Rev.-Sci. Eng.* **28**, 13 (1986).
2. Umbach, E., and Menzel, D., *Chem. Phys. Lett.* **84**, 491 (1981).
3. Avery, N. R., *Surf. Sci.* **131**, 501 (1983).
4. Cornish, J. C. L., and Avery, N. R., *Surf. Sci.* **235**, 209 (1990).
5. Li, Y., and Bowker, M., *Surf. Sci.* **348**, 67 (1996).
6. Vaterlein, P., Krause, T., Bassler, M., Fink, R., Umbach, E., Taborski, J., Wustenhagen, V., and Wurth, V., *Phys. Rev. Lett.* **76**, 4749 (1996).
7. Hoffman, D. A., and Hudson, J. B., *Surf. Sci.* **180**, 77 (1987).
8. Sau, R., and Hudson, J. B., *J. Vac. Sci. Technol.* **18**, 607 (1981).
9. Somorjai, G. A., "Introduction to Surface Chemistry and Catalysis." Wiley, New York, 1994.
10. Orita, H., Kondoh, H., and Nozoye, H., *J. Phys. Chem.* **99**, 3648 (1995).
11. Orita, H., Kondoh, H., and Nozoye, H., *Chem. Phys. Lett.* **228**, 385 (1994).
12. Kodama, C., Orita, H., and Nozoye, H., *Appl. Surf. Sci.* **121/122**, 579 (1997).
13. Besenbacher, F., and Norskov, J. K., *Prog. Surf. Sci.* **44**, 5 (1993).
14. Nozoye, H., *J. Phys. Chem.* **91**, 5087 (1987).
15. Winkler, A., and Rendulic, K. D., *Surf. Sci.* **118**, 19 (1982).
16. Erley, W., and Wagner, H., *Surf. Sci.* **74**, 333 (1978).
17. List, F. A., and Blakely, J. M., *Mat. Lett.* **1**, 95 (1982).
18. Cooper, E., Coats, A. M., and Raval, R., *J. Chem. Soc. Faraday Trans.* **91**, 3703 (1995).
19. Nozoye, H., *Chem. Lett.*, 1429 (1986).
20. Sueyoshi, T., Sasaki, T., and Iwasawa, Y., *Surf. Sci.* **343**, 1 (1995).